HAL
open science

Flux measurements in the near surface layer over a non-uniform crop surface in China

Z. Gao, L. Bian, S. Liu

To cite this version:

Z. Gao, L. Bian, S. Liu. Flux measurements in the near surface layer over a non-uniform crop surface in China. Hydrology and Earth System Sciences Discussions, 2005, 2 (3), pp.1067-1085. hal-00298666

HAL Id: hal-00298666

https://hal.science/hal-00298666v1

Submitted on 18 Jun 2008

HAL is a multi-disciplinary open access archive for the deposit and dissemination of scientific research documents, whether they are published or not. The documents may come from teaching and research institutions in France or abroad, or from public or private research centers.

L'archive ouverte pluridisciplinaire **HAL**, est destinée au dépôt et à la diffusion de documents scientifiques de niveau recherche, publiés ou non, émanant des établissements d'enseignement et de recherche français ou étrangers, des laboratoires publics ou privés.

Hydrol. Earth Sys. Sci. Discuss., 2, 1067–1085, 2005
www.copernicus.org/EGU/hess/hessd/2/1067/
SRef-ID: 1812-2116/hessd/2005-2-1067
European Geosciences Union

Hydrology and Earth System Sciences Discussions

Papers published in *Hydrology and Earth System Sciences Discussions* are under open-access review for the journal *Hydrology and Earth System Sciences*

Flux measurements in the near surface layer over a non-uniform crop surface in China

Z. Gao[1,2,3], L. Bian[1], and S. Liu[2]

[1]Chinese Academy of Meteorological Science, Beijing, China
[2]State Key Laboratory of Remote Sensing Science, School of Geography, Beijing Normal University, Beijing, China
[3]Jiangsu Province Key Laboratory of Meteorological Disaster and Environmental Variation, Nanjing, China

Received: 2 May 2005 – Accepted: 26 May 2005 – Published: 14 June 2005

Correspondence to: Z. Gao (zgao@cams.cma.gov.cn)

© 2005 Author(s). This work is licensed under a Creative Commons License.

Abstract

Eddy covariance measurements were conducted on fluxes of moisture, heat and CO_2 in a near-surface layer over a non-uniform crop surface in an agricultural ecosystem in the central plain of China from 10 June to 20 July 2002. During this period, the mean canopy height was about 0.50 m. The study site consisted of grass (10% of area), bean (15%), corn (15%) and rice (60%). Based on footprint analysis, we expected >90% of the measured flux (at a height of 4 m above ground surface) to occur within the nearest 600 m of upwind area. We examined interdiurnal variations in the components of the surface energy balance and in CO_2 flux. Results show that the pattern of energy partition had no obvious variation during the season. Daytime absorption of CO_2 flux by the crop canopy suddenly increased after thunderstorm events. We examined the energy budget closure and found it to be around 0.85. We compared energy partitioning for all rain-free days, and found energy imbalance was more significant for the 1∼3 days after rainy events and energy components almost achieve balance for the other rain-free days. It indicated that the cold or warm rainwater infiltrating into soil made problems.

1. Introduction

The direct and indirect effects of increasing atmospheric CO_2 may have profound implications for the structure and function of plant communities. Vegetation, in turn, plays a crucial role in the global carbon balance (Woodward et al., 1998; Mielnick et al., 2001). Climate simulations are especially sensitive to the surface partitioning of available energy into sensible and latent heat fluxes (e.g. Dickinson et al., 1991). Land surface processes are also critical in mesoscale atmospheric modeling (Chen and Dudhia, 2001; Sridhar et al., 2002). Agricultural ecosystem is one of the most widespread vegetation types in the world and therefore is a significant component of the earth's climate system. Many researchers have reported the direct measurements of surface energy components and CO_2 flux over homogenous crop surfaces (e.g. Harazono et al., 1998;

Miyata et al., 2000; Gao et al., 2003). However, in Asia, if an agricultural region is larger than 5 km×5 km, it must be non-uniform. It is especially true in China where farmers individually determine which type of crop for their rented fields. On the other hand, because climate and mesoscale modelers need to better parameterize near surface fluxes in their models, and researchers who devote interests to surface flux estimate from satellite strongly need to improve current retrieval algorithms, they all need accurate fluxes measured at the surfaces which represent large landscapes well. Field studies designed to characterize land surface processes in agricultural ecosystem are thus needed. To improve the current understanding of energy partitioning and CO_2 exchange in the main agricultural ecosystem in China, we conducted an intensive non-uniform surface experiment in China's Anhui province from 10 June to 20 July 2002. The site is typical of plains in central China. The objective of this note is therefore to present measurement results obtained in this micrometeorological field study.

2. Materials and methods

2.1. Site

The experiment was carried out at a conventional meteorological site (31°41′ N, 117°08′ E) in the main agricultural ecosystem of China during the period from 10 June to 20 July 2002. Soil at the experimental site was predominantly clay loam. The site surface was non-uniform, and consisted of grass (10%), bean (15%), corn (15%), and rice (60%) around. The predominant wind direction was south-east during the period of the experiment. On 6 June 2002 the micrometeorological instrumentation was set up. During the experiment the rice canopy height increased from 0.16 m to 0.65 m and the rice field was flooded throughout the entire experiment. The grass canopy height was 0.1 m; bean height increased from 0.3 m to 0.55 m; and corn height increased from 0.3 m to 1.2 m.

2.2. Micrometeorological measurements

A three-dimensional ultrasonic anemometer (CSAT3, Campbell Scientific Inc.) was used to measure the means and standard deviations of the wind velocity components (i.e. u, v and w); a Krypton hygrometer (KH20, Campbell Scientific Inc.) was used to measure the mean and standard deviation of water vapor density; and a fine-wire thermocouple (FW05) was used to measure the mean and standard deviation of air temperature. These sensors were installed at 4.0 m above the ground surface. All signals for the sensors were recorded at a sampling rate of 20 Hz and were averaged over 30 min periods.

Webb et al. (1980) showed that the eddy flux of heat should be calculated using the heat capacity of moist air and the covariance between temperature and vertical wind speed, and that corrections are needed for density fluctuations in calculating the fluxes of water vapor and CO_2. So we corrected the latent heat flux for the variation in air density owing to the transfer of sensible heat, and corrected the sensible heat flux for the variation in air density owing to the latent heat flux. Webb et al. (1980) corrections were also used for CO_2 flux. Following Moore (1986), we corrected eddy covariance values for the effects of path length averaging of the sonic anemometer and the gas analyzer, and for spatial separation of sensors.

The ultrasonic anemometer was tested for accuracy in the wind tunnel at the Metering Station of the China Meteorological Administration and found that they gave consistent results. The measured composite horizontal winds differed systematically by only ~1% from the actual wind, although the differences were larger at speeds $<0.5\,\mathrm{ms}^{-1}$. During the fieldwork we compared the output voltage V from the infrared hygrometer (E009B) to the specific humidity q in various bands of specific humidity and found that V was a linear function of q.

We eliminated noise and various kinds of interference from the 30-min measurements of turbulence by using a criterion of $X(t)<(\overline{X}-4\sigma)$ or $X(t)>(\overline{X}+4\sigma)$, where $X(t)$ denotes the measurement (i.e. wind speed, temperature), $\overline{X}$ the mean over the interval,

and σ the standard deviation. We interpolated by averaging the sample immediately before the sample to be removed with the one immediately after it. Data during precipitation events was removed because the sonic anemometer and Krypton hygrometer would not give accurate results under such conditions.

The set of observational data includes these meteorological quantities: horizontal wind speed, air temperature, specific humidity, CO_2 density and precipitation. These data were collected at the height of 4.0 m above water. As shown in Fig. 1, air temperature and CO_2 density undergo a marked diurnal cycle, but they have contrary phases. It must be noted that in the period selected there are a lot of gaps that were caused by rainy events. Two thunderstorm events happened during our experiential period. One is for the period from 02:00 to 10:00 (LT) on DOY 175 (i.e. 24 June), and the maximum precipitation intensity reached 25.5 mm h^{-1}; the other is for the period from 13:00 to 17:00 (LT) on DOY 178 (i.e. 27 June), and the maximum precipitation intensity reached 41.1 mm h^{-1}.

Gao et al. (2003) investigated the aerodynamic roughness length (z_0) and zero plane displacement (d) of a rice paddy under different conditions. They found that z_0 and d are 0.027 m and 0.43 m respectively, and z_0 increased with increasing wind speed when the height of the rice was >0.5 m. In this study, we assumed that $d \approx 3h/4$, where h is the canopy height, which was determined by an area-weight average for upwind area (wind direction ±30°). The average surface roughness length z_0 of approximately 0.024 m was derived from the ultrasonic anemometer data under near neutral conditions (Katul et al., 1995) for our experimental period.

2.3. Flux computations

Surface energy balance in an agricultural crop surface can be approximated as

$$Rn = H + LE + G_0 , \quad (1)$$

where Rn, H, LE and G_0 are the net radiation, sensible heat, latent heat and soil heat fluxes respectively. Eddy fluxes of sensible heat and latent heat were computed as

(e.g. Kaimal and Finnigan, 1994):

$$H = \overline{\rho} C_p \overline{w'T'}, \tag{2}$$

$$LE = L\overline{\rho}\overline{w'q'}, \tag{3}$$

where $\overline{\rho}$, C_p and L are the density of air (kg m^{-3}), the specific heat of air (J kg^{-1} K^{-1}), and latent heat of vaporization (J kg^{-1}), respectively. w', T' and q' are the fluctuations of vertical wind component (m s^{-1}), air temperature (K) and specific humidity, respectively.

With no other sources/sinks of heat in the soil at our site, the surface soil heat flux (G_0) was calculated as:

$$G_0 = G_1 + C_s \Delta z' \partial T_s / \partial t, \tag{4}$$

where G_1 is the soil heat flux measured at 0.05 m below the soil surface (W m^{-2}); C_s is the volumetric heat capacity of soil (2.42×10^6 J m^{-3} K^{-1}, Stull, 1988), $\Delta z'$=0.05 m, and T_s is the mean temperature of 0–0.05 m soil layer, calculated from the temperatures measured at surface and at 0.05 m depth.

Net radiation (Rn) can be obtained by

$$Rn = ISR + ILR - OSR - OLR, \tag{5}$$

where ISR and ILR are downward short- and long-wave radiation, OSR and OLR are upwelling reflected short-wave radiation and long-wave radiation emitted by surface, respectively.

Since the 1980s, the development of fast response CO_2 analyzers enabled us to directly measure CO_2 fluxes over rice canopies using eddy covariance methods. Ohtaki and Matsui (1982) and Ohtaki (1984) defined the following equation to reliably estimate CO_2 flux:

$$F_{CO_2} = \overline{w'c'}, \tag{6}$$

where F_{CO_2} is CO_2 flux (mg m^{-2} s^{-1}), c' is the fluctuation in the concentration of CO_2 (mg m^{-3}).

2.4. Fetch analysis

The adequacy of the fetch may be confirmed by footprint analysis (e.g. Schuepp et al., 1990; Harazono et al., 1998). The cumulative normalized contribution to the surface flux from upwind locations, $C_F(\chi_L)$, can be expressed as

$$C_F(\chi_L) = e^{-U(z-d)/(ku_*\chi_L)}, \tag{7}$$

where d is the zero plane displacement, k is von Karman's constant, u_* is the friction velocity, χ_L is the distance upwind of the measuring point, and U is the average wind speed between the surface and observation height z. Assuming a logarithmic profile for horizontal wind speed $u(z)$, with z, U is given by

$$U = \int_{d+z_0}^{z} u(z)dz \Big/ \int_{d+z_0}^{z} dz = \frac{u_*[\ln((z-d)/z_0^{)} - 1 + z_0/(z-d)]}{k(1-z_0/(z-d))}.$$

3. Results and discussion

3.1. Fetch analysis

Data were collected at 4.0 m above the ground surface, which was well above the canopy ($z>3h$, where h is the crop canopy height) and thus the flow assumes the inertial sub layer properties of the conventional atmospheric surface layer such as the constant flux region. To estimate the average footprint for whole observational period, where d=0.37 m on average, the contributions of the cumulative flux were computed using Eq. (7). Our analysis, shown in Fig. 2, indicates that approximately 90% of

the measured flux at the measurement height was expected to come from within the nearest 600 m of upwind area for neutral stability during the entire period.

3.2. Variations throughout the entire experiment

3.2.1. Radiation balance components

The measured interdiurnal variations of surface radiation components at a height of 1.5 m at our site from 10 June to 20 July 2002 are shown in Fig. 3, where coinstantaneous precipitation (prec.) distribution is also given. It can be seen that all components of radiation fluxes varied diurnally, and downward shortwave radiation (DSR) flux was strong and the daily peak often exceeded 700 Wm^{-2} around noon during clear days. A large amount of solar energy can be received by the surface as the albedo (0.17) is low. This value (0.17) agrees with the representative value (0.15–0.25) of short-wave albedo for crop surfaces (Garratt, 1992). We note that, owing to the cloud existence, downward shortwave radiation flux, upward shortwave radiation (USR) flux and upward long-wave radiation (ULR) flux were significant low, and downward long-wave radiation (DLR) flux was high during rainy period. Net radiation can be derived by radiation budget as shown in Fig. 4. We can regard net radiation (Rn) as an external force, while the sensible flux (H), latent flux (LE), and ground flux (G_0) are the responses.

3.2.2. Energy balance components

Figure 4 illustrates the time series of energy budget components obtained by direct measurements for the entire experimental period. Our analyses on the surface energy balance in this section are focused on the data collected on clear days (i.e. DOYs: 162–163, 165, 169, 177, 183, 188–195, and 200), because the sonic anemometer and Krypton hygrometer would be in error during and after rain events, and the cold or warm rainwater infiltrating into soil would create complexities. The diurnal patterns of Rn, H, LE and G_0 barely changed for these clear days, indicating that the energy

partition barely changed. The maximum value of Rn was ~600 W m^{-2}, the maximum value of LE reached 229 W m^{-2}, the maximum value of H was 145 W m^{-2}, and the maximum value of G_0 was 215 W m^{-2}on the basis of direct measurements. The Bowen ratio β ($\beta \equiv H/LE$), on average, was 0.49 for our experimental period.

3.2.3. CO_2 flux

The interdiurnal course of CO_2 fluxes above the canopy measured by the eddy covariance method is shown in Fig. 4, where a negative sign denotes downward and means the canopy absorbed CO_2 from the atmosphere. In contrast to energy partition mentioned above, CO_2 flux (F_{CO_2}) absorbed by the canopy suddenly increased after thunderstorm events, as shown in Fig. 4. This was likely caused by quick growth of crop canopy which changed both leaf area index (LAI) and photosynthetically active radiation. The maximum value of CO_2 flux absorbed by crop canopy was 0.81×10^{-6} kg m^{-2} s^{-1} during our experimental period. It is about half of that obtained over a pure rice paddy (Gao et al., 2003). This difference is likely caused by the different both leaf area index (LAI) and photosynthetically active radiation for two different surfaces.

3.2.4. Soil temperature and soil volume water content

Figure 5a shows the time series of soil temperatures at ground surface and at three depths in the soil covered by short grass. It is apparent that soil temperature, in shallow surface layer, responded to solar radiation, precipitation and soil volume water content sensitively. Figure 5b shows the time series of the soil volume water content obtained by direct measurements in 0–0.15 m surface layer and 0.15–0.30 m soil layer in the soil covered by grass at our site. Figure 5c shows the time series of the precipitation. We find that (a) in both two soil layers, soil volume water content responded to precipitation sensitively with the most striking cases happened on DOYs 161, 170, 171, 174, 178, and 179, when a thunderstorm made the greatest sudden change of soil wetness; and (b) soil volume water content gradually decreased owing to evaporation from bare soil

surface and the transpiration of canopy since DOY 180.

3.3. Energy budget closure

Surface energy budget closure, ε, defined as the ratio of the sum of sensible and latent heat fluxes ($H+LE$) to available energy (the difference of net radiation and soil heat flux: $Rn-G_0$) (Gu et al., 1999), has been prescribed to examine the surface energy balance. Ideally, ε should be equal to one, when the surface energy balance (i.e. partitioning of Rn into H, LE, and G_0) is perfectly closed. Figure 6 gives the inter-comparison of $H+LE$ and available energy ($Rn-G_0$). It is found that the mean value of energy budget closure (ε) is about 0.85. To clarify on which days energy imbalance were more significant for all rain-free days, we plot the bar graph of all daily averaged energy components and residual energy ($Re \equiv Rn-H-LE-G_0$) in Fig. 7. It is obvious that the energy imbalance was significant during the 1∼3 days after rain events (i.e. DOYs 162–163, 176–177, 182–183, 189–191, and 200), and energy components almost achieved balance for other rain-free days.

4. Summary and conclusions

In this paper we have reported our measurements of the energy budget components and CO_2 exchange over a non-uniform crop surface in an agricultural ecosystem in China from 10 June to 20 July 2002.

Daily patterns of latent heat (LE), sensible heat flux (H), surface heat flux (G_0) and CO_2 flux (contrary phase) followed that of net radiation (Rn).

The energy closure ratio (ε) averaged 0.85 during the experiment, and energy imbalance mainly happened during the 1∼3 days after rain events. So we concluded that the cold or warm rainwater infiltrating into soil made problems. Meanwhile, energy components almost achieved balance for other rain-free days. Hence, our flux data are of sufficiently good quality not only for quantification but also for other applications

such as model validation and calibration.

Main new finding of this research is that, with the crop growth, the pattern of energy partition and the magnitude of energy budget components remained fairly constant. The energy closure ratio (ε) had no obvious variation during the experiment. In contrast, crop canopy absorbed more CO_2 during the daytime with the crop growth. The maximum value of CO_2 flux absorbed by canopy was 0.81×10^{-6} kg m^{-2} s^{-1} during our experimental period.

Acknowledgements. This study was financially supported by the National Key Basic Research and Development Project of China through Research on Theories and Methods of Monitoring and Predicting of Heavy Rainfall in South China (2004CB418300). Special thanks to L. Lu, X. Wang and C. Lu for their support in field data collection.

References

Chen F., and J. Dudhia, Coupling an advanced land-surface/hydrology model with the Penn State-NCAR MM5 modeling system, part I, Model implementation and sensitivity, Mon. Weather Rev., 129, 569–582, 2001.

Dickinson, R. E., Hendersin-Sellers, A., Rosenzweig, C., and Sellers, P. J.: "Evapotranspiration models with canopy resistance for use in climate models, a review", Agric. For. Meteorol., 54, 373–388, 1991.

Garratt, J. R.: The Atmospheric Boundary Layer, Cambridge University Press, New York, USA, 291–292, 1992.

Gao, Z., Bian, L., and Zhou, X.: Measurements of Turbulent Transfer in the Near-surface Layer over a Rice Paddy in China, J. Geophys. Res., 108, D13, 4387, dio:10.1029/2002JD002779, 2003.

Harazono, Y., Kim, J., Miyata, A., Choi, T., Yun, J.-I., and Kim, J.-W.: Measurement of energy budget components during the International Rice Experiment (IREX) in Japan, Hydrological Processes, 12, 2018–2092, 1998.

Kaimal. J. C. and Finnigan, J. J.: Atmospheric boundary layer and flows, Oxford University Press, 289, 1994.

Katul, G. G., Goltz, S. M., Hsieh, C.-I., Cheng, Y., Mowry, F., and Sigmon, J.: Estimation of surface heat and momentum fluxes using the flux-variance method above uniform and non-uniform terrain, Bound.-Layer Meteorol., 74, 237–260, 1995.

Mielnick, P. C., Dugas, W. A., Johnson, H. B., Polley, H. W., and Sanabria, J.: Net grassland carbon flux over a subambient to superambient CO_2 gradient, Global Change Biology, 7, 747–754, 2001.

Miyata, A., Leuning, R., Denmead, O. T., Kim, J., and Harazono, Y.: Carbon dioxide and methane fluxes from an intermittently flooded paddy field, Agricultural and Forest Meteorology, 102, 287–303, 2000.

Moore, C. J.: Frequency response to corrections for eddy correlation system, Bound.-Layer Meteor., 37, 17–35, 1986.

Ohtaki, E.: Application of an inferred carbon dioxide and humidity instrument to studies of turbulent transport, Bound.-Layer Meteor., 29, 85–107, 1984.

Ohtaki, E. and Matsui, T.: Infrared device for simultaneous measurement of atmospheric carbon dioxide and water vapor, Bound.-Layer Meteor., 24, 109–119, 1982.

Schuepp, P. H., Leclerc, M. Y., MacPherson, J. I., and Desjardins, R. L.: Footprint prediction of scalar fluxes from analytical solution of the diffusion equation, Bound.-Layer Meteor., 50, 355–373, 1990.

Sridhar, V., Elliott, R. L., Chen, F., and Brotzge, J. A.: Validation of the NOAH-OSU land surface model using surface flux measurements in Oklahoma, J. Geophys. Res., 107, D20, 4418, dio:10.1029/2001JD001306, 2002.

Stull, R. B.: An Introduction to Boundary Layer Meteorology, Kluwer Acad., Norwell Mass., 274–287, 1988.

Webb, E. K., Perman, G. I., and Leuning, R.: Correction of flux measurements for density effects due to heat and water transfer, Quart, J. Roy. Meteor. Soc., 106, 85–100, 1980.

Woodward, F. L., Lomas, M. R., and Betts, R. A.: Vegetation-climate feedbacks in a greenhouse world, Philosophical Transactions of the Royal Society, London, 353, 29–39, 1998.

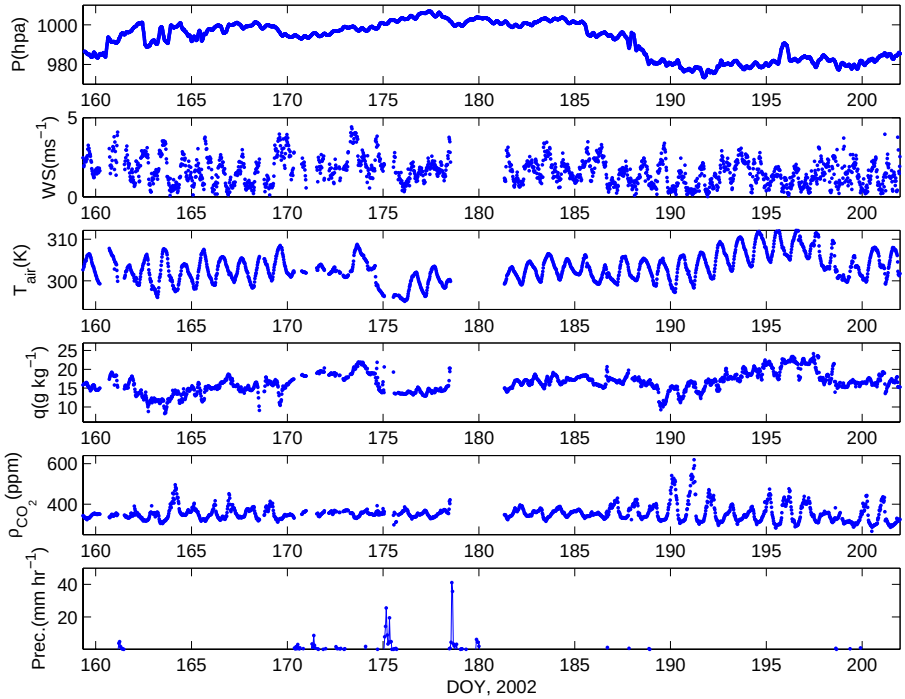

Fig. 1. Hourly meteorological data for 10 June to 20 July 2002 over a non-uniform crop surface.

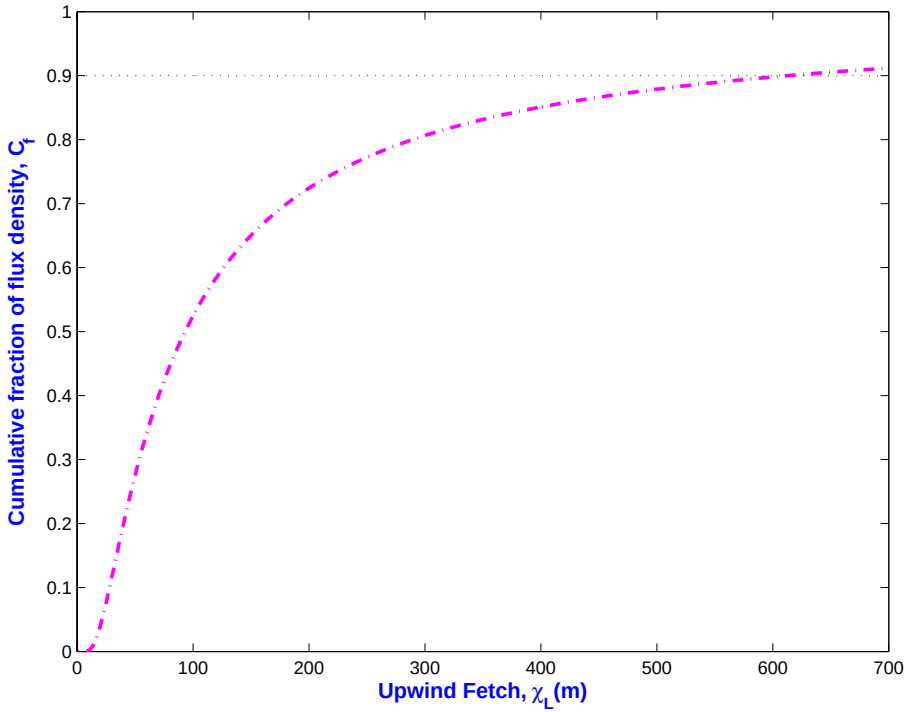

Fig. 2. Contribution of the cumulative flux, according to Eq. (7) for neutral stability of the experiment period.

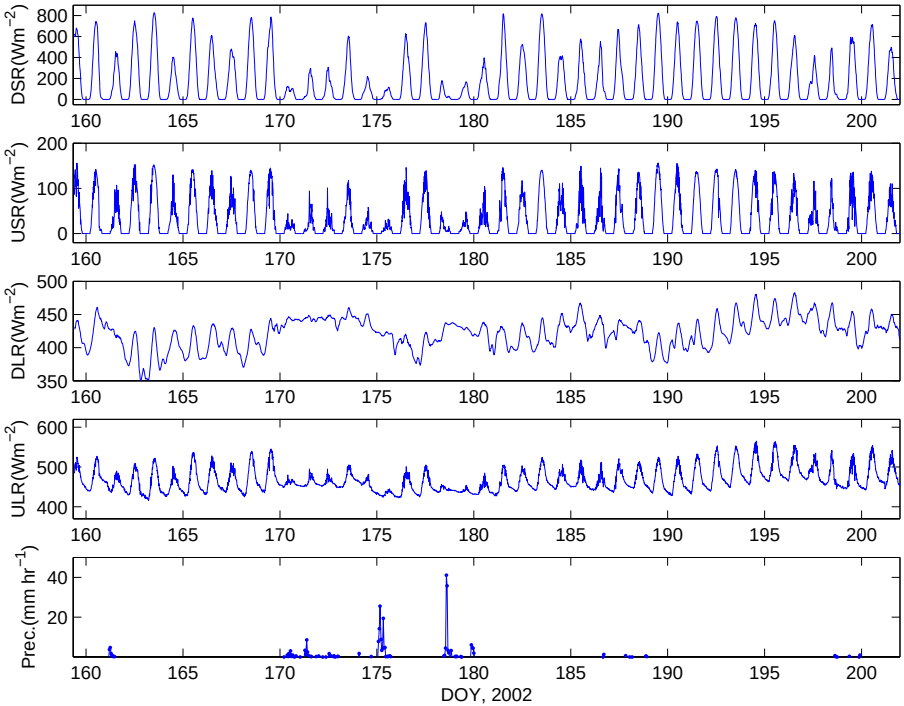

Fig. 3. Variation of downward shortwave radiation (*DSR*), upward shortwave radiation (*USR*), downward longwave radiation (*DLR*) and upward longwave radiation (*ULR*) fluxes and precipitation (Prec.) from 10 June to 20 July 2002 over a non-uniform crop surface.

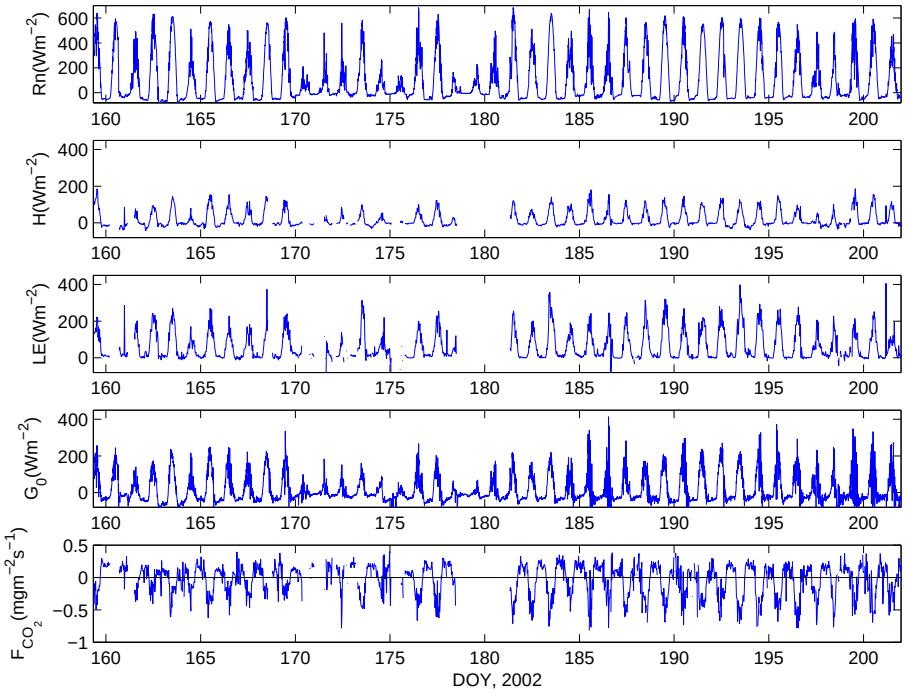

Fig. 4. Variation of net radiation (Rn), sensible heat (H), latent heat (LE), soil heat (G_0), and CO_2 flux (F_{CO_2}) from 10 June to 20 July 2002 over a non-uniform crop surface.

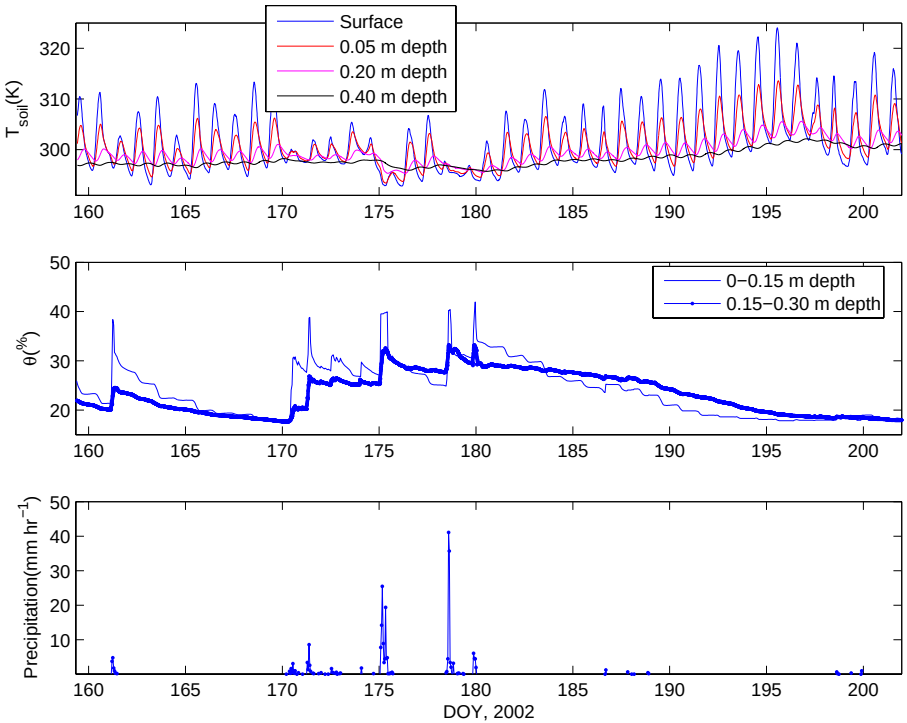

Fig. 5. Variation of soil temperature at four depths, and soil volume water content from 10 June to 20 July 2002 over a non-uniform crop surface.

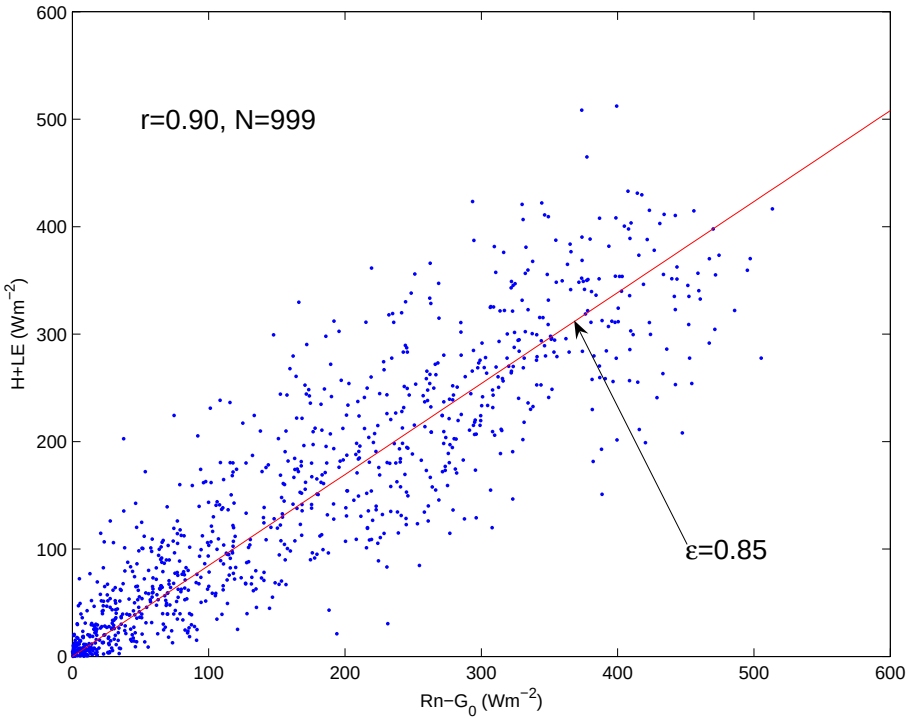

Fig. 6. Comparison of sum of sensible heat and latent heat fluxes (H+LE) and available energy ($Rn-G_0$) for rain-free days during our experimental period.

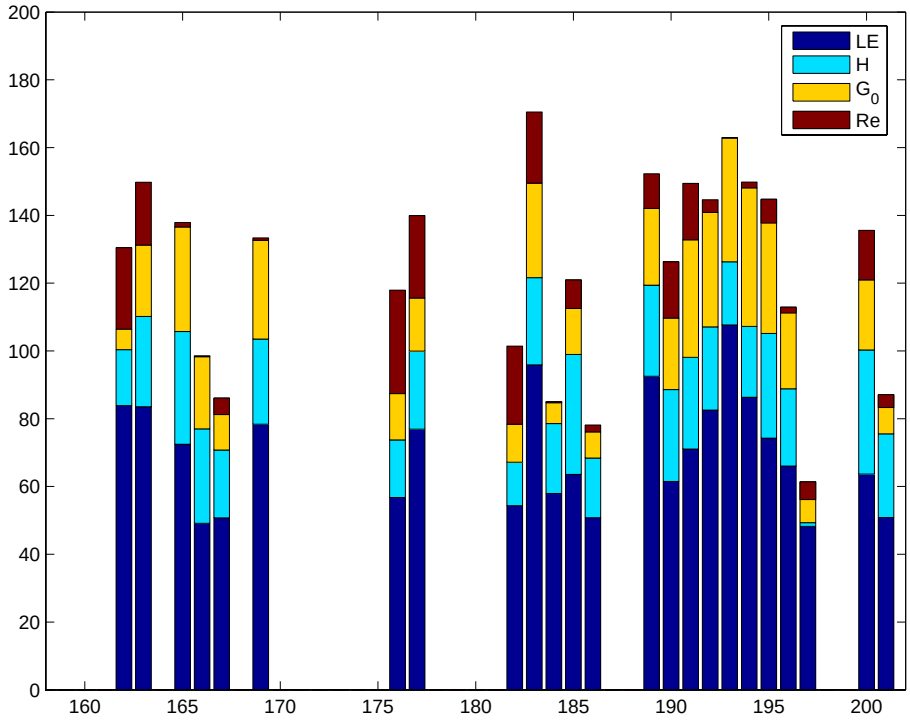

Fig. 7. Bar plots of daily averaged latent heat flux (LE), sensible heat flux (H), soil heat flux (G_0) and residual energy (Re) for rain-free days during our experimental period.